The thinnest of all the viscous layers examined above is induced on their surfaces for the flow around the roughnesses (6.1) (''thick'' in the terminology of [2]). Hence, domains 2 and 1 are perturbed only by the shape of the roughness, and in this case the Prandtl spatial boundary layer equations with a given pressure distribution must be solved (the boundary value problem (5.2), (5.3), (5.9), (6.2), (6.5), and (6.6), the line HI in Fig. 2).

It is obtained in [2] that because of the diminution of the transverse velocity component w in order of magnitude during passage from the flow around non-narrow roughnesses ($c \sim b$) on a flat plate to narrow ($c < b$) the perturbation transmission upstream disappears for them. If the roughness is on a curved surface, then Δp_1 and Δp_2 have identical signs for a concave surface and different signs for a convex. Consequently, for narrow roughnesses on a concave surface the total pressure perturbation is greater than for roughnesses on a flat surface. This results in an increase in the transverse velocity component w and the origination of upstream perturbation transmission [3, 4]. For roughnesses on convex surfaces such a phenomenon should not be realized.

LITERATURE CITED

1. G. R. Hough (ed.), Viscous Flow Drag Reduction. Symposium on Viscous Drag Reduction. Dallas, Texas (1979).
2. V. V. Bogolepov, ''General scheme of spatial local flow regimes,'' Prikl Mekh. Tekh. Fiz., No. 6 (1986).
3. S. B. Rozhko and A. I. Ruban, ''Longitudinal—transverse interaction in three-dimensional boundary layer,'' Izv. Akad. Nauk SSSR, Mekh. Zhidk. Gaza, No. 3 (1987).
4. S. B. Rozhko, A. I. Ruban, and S. N. Timoshin, ''Spatial boundary layer interaction with an extended obstacle,'' Izv. Akad. Nauk SSSR, Mekh. Zhidk. Gaza, No. 1 (1988).

STEADY SURFACING OF A SINGLE BUBBLE IN AN INFINITE VOLUME OF LIQUID

P. K. Volkov and E. A. Chinnov

UDC 532.529.6

The motion of individual gas bubbles has long been an object of investigation. Important theoretical solutions have been obtained and a sizable body of experimental data has been accumulated. Recent years have seen the broad use of numerical methods to solve the Navier—Stokes equations with an unknown boundary in regard to the study of bubble motion [1, 2].

Here, we use numerical solutions that we obtained to the complete Navier—Stokes equations and the results of an experiment to analyze the simultaneous effect of the viscosity of the liquid and surface tension on the rate of surfacing and form of individual bubbles. We also determine the limits of disturbance of the sphericity of gas bubbles and the formation of eddies in the rear part of the bubbles.

We examine the steady surfacing of an axisymmetric bubble with the boundary Γ. The volume of the bubble is constant, as is the pressure inside it. We introduce cartesian coordinate system x_1, x_2, x_3, connected with the center of the bubble. The x_3 axis is directed along the upward velocity of the gas cavity, $\mathbf{u}$, $\mathbf{n}$ is the unit vector of an outward normal to Γ, τ is the unit vector of a tangent to Γ. The motion of the viscous liquid outside the closed surface Γ is described by the system of equations

$$(\mathbf{v}\nabla)\mathbf{v} + \nabla p/\rho = \nu\Delta\mathbf{v}, \quad \nabla\mathbf{v} = 0, \tag{1}$$

where p is the modified pressure function: $p = q + \rho g x_3 - p_0$; q is the pressure in the liquid; p_0 is the pressure at the level $x_3 = 0$; g is acceleration due to gravity; ρ is the density of the liquid; ν is the kinematic viscosity of the liquid.

The following conditions are satisfied on the free boundary Γ: impermeability

Novosibirsk. Translated from Zhurnal Prikladnoi Mekhaniki i Tekhnicheskoi Fiziki, No. 1, pp. 94-99, January-February, 1989. Original article submitted October 27, 1987.

0021-8944/89/3001-0089$12.50

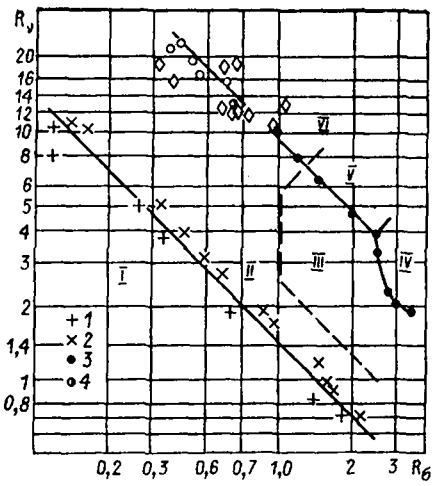

Fig. 1

$$\mathbf{v}\cdot\mathbf{n} = 0; \tag{2}$$

triviality of the shear stresses in the liquid

$$\boldsymbol{\tau}\cdot T\cdot\mathbf{n} = 0; \tag{3}$$

equality of the difference of the normal stresses on the bubble surface to the capillary pressure σK

$$p - 2\rho\nu(\mathbf{n}\cdot T\cdot\mathbf{n}) + \sigma K = p_g - p_0 + g\rho x_3. \tag{4}$$

Here, $T_{ij} = \frac{1}{2}\left(\frac{\partial v_i}{\partial x_j} + \frac{\partial v_j}{\partial x_i}\right)$ is the strain-rate tensor; p_g is the pressure of the gas in the bubble; K is the curvature of the surface Γ; σ is surface tension.

At infinity

$$\mathbf{v} = -\mathbf{u}. \tag{5}$$

Problem (1)-(5) is solved numerically in the variables curl ω—stream function ψ. The problem is solved by the iteration method using a scheme that employs a stabilizing correction. The algorithm was examined in detail in [1, 2]. Problem (1)-(5) contains the following parameters which are important for the process being examined: ρ, ν, σ, g, R, $p_g - p_0$, u (R is the radius of a sphere equivalent in volume to the bubble).

It should be noted that the solution depends only on the difference between the pressures $p_g - p_0$. It is also evident that we cannot arbitrarily assign R and $p_g - p_0$ in the given liquid, since it follows from (4) with u = 0 and g = 0 that we have a spherical bubble and

$$2\sigma/R = p_g - p_0 \tag{6}$$

for any ρ and ν. Five of the above seven quantities are independent and, in accordance with dimensional theory, there are two independent dimensionless parameters. Since the choice of the determining variables is to a certain extent arbitrary, different dimensionless criteria are used when examining the motion of individual bubbles. At first glance, the use of the length scale $L = \sigma/(p_g - p_0)$ (following [1]) avoids the difficulties connected with the fact that (1) contains the pressure gradient p. However, in the numerical solution, the fact that (4) contains the function p — which is calculated with the integration of (1) — makes it necessary to unambiguously determine this function. This can be done as follows. With allowance for the choice of L, it follows from (6) that R ≡ 2L (which corresponds to the solution of (4) with We = 0, $We = \rho Lu^2/\sigma$). We find the stream function and the curl and we determine p from (1). Since the liquid and the bubble are in equilibrium, then the integral of p over the bubble surface must be equal to zero. This condition allows us to find p_0 and, thus, the pressure function.

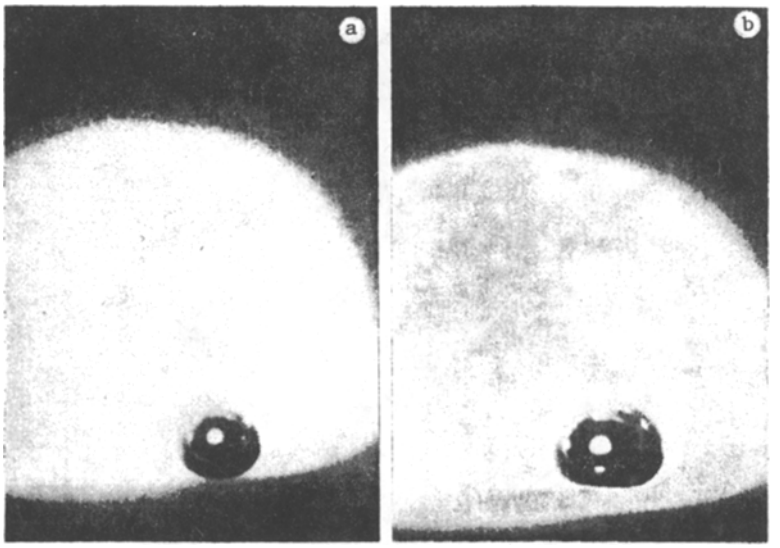

Fig. 2

The quantities Re* (Re* = uL/ν) and We were used in [2] as the determining criteria, Re = 2uR/ν, E = $4\rho gR^2/\sigma$, were used in [3], while the authors of [4] proposed the use of the criteria M = $\rho^3\nu^4 g/\sigma^3$, R/R_o (R_o = $[\sigma\nu^2/(\rho g^2)]^{1/5}$).

The choice of criteria for analyzing bubble motion depends mainly on how convenient their use is for obtaining information of practical importance on the process and how simply they allow the process to be described.

In practice, flow-rate characteristics of the process are commonly used. In the present case, we are employing the volume of the bubble or its equivalent radius R. As it has turned out [5-7], it is convenient to use the following characteristic scales to describe the motion of gas—liquid systems: $\delta_\nu = (\nu^2/g)^{1/3}$ — the viscous-gravitational interaction constant; $\delta_\sigma = [\sigma/(\rho g)]^{0.5}$ — the capillary constant. If we relate these scales to the characteristic dimension of the problem, we can determine the degree to which a given type of interaction occurs in the given process. Thus, we have two determining criteria: $R_\nu = \frac{R}{\delta_\nu} = \left[\frac{(\rho u^2)(g\rho R)}{(\nu\rho u/R)^2}\right]^{1/3} = (\mathrm{Re}/2\mathrm{Ps})^{1/3}$ shows the relative effect of inertial forces in the liquid, molecular friction, and ejection and is a unique analog of the Reynolds number for processes in which motion is due to buoyancy (Ps = vu/gR^2); $R_\sigma = \frac{R}{\delta_\sigma} = \left[\frac{\rho gR}{\sigma/R}\right] = \frac{1}{2}\sqrt{E}$ characterizes the relative effect of buoyancy and surface tension. These criteria have two important properties. First, they do not contain bubble velocity. Second, their ratio represents a complex which consists only of physical characteristics of the medium:

$$R_\sigma/R_\nu = \delta_\nu/\delta_\sigma = (\rho^3\nu^4 g/\sigma^3)^{1/6} = \mathrm{M}^{1/6}.$$

These properties simplify the description of the process considerably. Thus, on a diagram with the coordinates R_ν and R_σ, lines representing constant values of M will be straight rather than curved (as in the diagram in [3]). The rate of surfacing of the bubble is contained only in the determining criterion (Fr = u^2/gR), which makes it possible to obtain information on it directly from the diagrams. A bubble surfacing in a liquid may take different forms, depending on the size and physical characteristics of the medium.

Figure 1 shows data on the surfacing of single bubbles in a diagram with the coordinates R_ν and R_σ. Here, we examine the change in the form of the bubbles and the formation of eddies behind them in the complex and little-studied transitional regions, where the effect of all of the determining parameters is substantial. Regions in which bubbles are present with a gas film in the form of a "skirt" and an open wake [8] are not indicated in the figure. The number I denotes the region in which the surfacing bubbles have a spherical form. The main characteristic defining the boundary of this region is the degree of deformation of the bubble e = $(a - b)/a$ (a is the horizontal dimension of the bubble and b is its vertical dimension). The diagram shows data from the numerical solution of problem

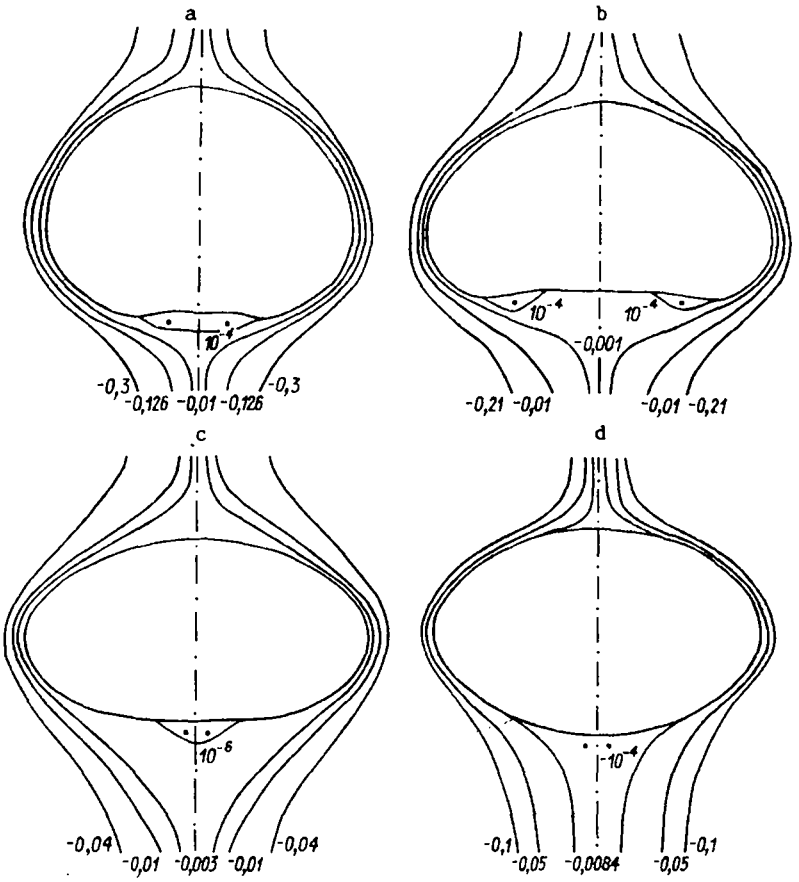

Fig. 3

(1)-(5) and from experiments (points 1), which indicate that the bubbles are deformed 0.5% (e = 0.005). Sphericity is considered to have been disturbed when the bubble deformation is greater than 1%. The diagram shows both numerical and empirical results corresponding to values of e in the 2-3% range (points 2). The solid line delineating the region I was determined by the expression $R_\nu R_\sigma = 1.4$.

Deformed bubbles can take different forms. The form of bubbles surfacing in water and other low-viscosity liquids is close to an ellipsoid of revolution [9, 10]. In more viscous media, the shape of bubbles is similar to an axisymmetric oblate ellipsoid (Fig. 2a, R_ν = 1.14, R_σ = 1.67). At $R_\sigma \geqslant 1$, $M \geqslant 3 \cdot 10^{-5}$, $R_\nu R_\sigma \geqslant 2.5$ (region III, Fig. 1), the symmetry of the surfacing bubble relative to the horizontal axis is disturbed. The dashed line constructed on the basis of the data we obtained indicates that the symmetry of the bubble is disturbed 3%. The characteristic form of the bubble satisfying these conditions is shown in Fig. 2b (R_ν = 1.5, R_σ = 2.15). Region III is a region of transition to region IV, where the bubbles are oblate ellipsoids. Region IV was examined in detail in [8]. In region III, the effect of surface tension begins to weaken ($R_n \geqslant 1$), but viscosity has not yet become the predominant factor in the bubble-surfacing mechanism [8].

Figure 1 shows the results of numerical solution of problem (1-5) (points 3), where we recorded the creation of an eddy in the rear part of the bubble. Some of these results are shown in Fig. 3. At R_σ = 3.0 and R_ν = 2.1 (Fig. 3a), an eddy is formed in the lower part of a bubble which is already quite nonsymmetrical relative to the horizontal axis. In this case, the form of the bubble is closer to a sphere than an oblate ellipsoid. The curve corresponding to the beginning of eddy formation at $R_\sigma \geqslant 2.5$ follows the dashed line indicating the disturbance of the symmetry of the bubble. This means that, in this case, the beginning of eddy formation behind the bubble depends to a considerable extent on the degree of its asymmetry.

At $R_\sigma < 2.5$, the numerical data corresponding to the creation of an eddy behind the bubble is represented by the solid line $R_\nu R_\sigma = 9$. It can be seen from Fig. 3, b-d (R_ν = 3.9;

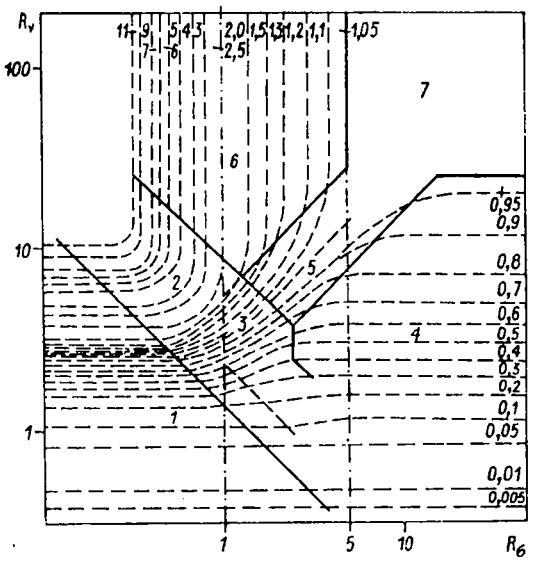

Fig. 4

6.3; 13.3 and R_σ = 2.4; 1.4; 0.64, respectively) that the bubbles are more oblate in this case. Meanwhile, at $M < 3 \cdot 10^{-5}$, the bubbles are symmetrical relative to the horizontal axis (d).

Whereas Fig. 3, a and c, shows the theoretical shapes of bubbles with an eddy in their lower part about the vertical symmetry axis, it is evident from Fig. 3b, corresponding to the inflection point on the solid curve, that the eddy is formed closer to the edges of the bubble. Thus, we can qualitatively distinguish three types of eddy formation behind a bubble and three corresponding regions IV-VI. In regions IV and V, the motion of bubbles is rectilinear and their shape is nonsymmetrical relative to the horizontal axis. At the boundary of region VI, the form of the bubbles is symmetrical. Figure 3d shows the results of numerical calculation of flow around a bubble before the formation of the eddy at its rear (point 4 in Fig. 1). In the calculation of such a bubble, the number of iterations increases sharply compared to the calculation of bubbles with smaller values of R_ν and R_σ. We were generally unsuccessful in advancing beyond this point, since a steady-state regime could not be established in the calculations with a further increase in R_σ. This is evidently related to the fact that the formation of an eddy in the rear of the bubble leads to loss of stability of the rectilinear motion. Figure 1 shows experimental data from [11] indicating the beginning of rectilinear motion of bubbles (points 5). The figure also shows our test data (points 6) corresponding to the motion of bubbles in a spiral.

Figure 4 shows the simultaneous effect of the criteria R_ν and R_σ on the dimensionless velocity (Froude number) of a bubble. Along with our data, the figure shows results from [12-15]. The designations of the bubble surfacing regimes corresponds to Fig. 1. The dashed curves correspond to constant values of Fr. In limiting cases of similarity with respect to one or two of the determining parameters (regions I, IV, VI, VII), the bubble surfacing law can be described by familiar relations. In transitional regions II, III, and V, the diagram in Fig. 4 can be used to evaluate Fr and, thus, the rate of bubble rise.

LITERATURE CITED

1. P. K. Volkov, "Numerical solution of a problem of the flow of a viscous liquid about a gas bubble," ChMMSS, 13, No. 1 (1982).
2. C. I. Christov and P. K. Volkov, "Numerical investigation of the steady viscous flow past a stationary deformable bubble," J. Fluid Mech., 158, 341 (1985).
3. I. R. Grace, "Shape and velocities of bubbles rising in infinite liquids," Trans. Inst. Chem. Eng., 51, 116 (1973).
4. O. V. Voinov and A. G. Petrov, "Motion of bubbles in a liquid," Itogi Nauki Tekh. Mekh. Zhidk. Gaza, 10, 86 (1976).
5. S. S. Kutateladze, Analysis of Similarity in Thermophysics [in Russian], Nauka, Novosibirsk (1982).

6. S. S. Kutateladze, I. G. Malenkov, and E. A. Chinnov, "Results of an experimental study of the effect of the walls of a vertical channel on the rate of rise of single bubbles of different sizes," in: Disperse Systems in Electrochemical Processes [in Russian], Inst. Teplofiz. Sib. Otd. Akad. Nauk SSSR, Novosibirsk (1982).
7. E. A. Chinnov, "Analysis of the surfacing of single bubbles in an infinite volume of liquid," in: Current Problems of Thermophysics [in Russian], Inst. Teplofiz. Sib. Otd. Akad. Nauk SSSR, Novosibirsk (1984).
8. D. Bhaga and M. B. Weber, "Bubbles in viscous liquids: shape, wakes, and velocities," J. Fluid Mech., 105, 61 (1981).
9. D. W. Moore, "The boundary layer on spherical gas bubbles," J. Fluid Mech., 16, No. 7 (1963).
10. W. L. Haberman and R. K. Morton, "An experimental study of bubbles moving in liquids," Proc. Am. Soc. Civ. Eng., 49, 387 (1954).
11. H. Tsuge and S. Hibino, "The onset conditions of oscillatory motion of single gas bubbles rising in various liquids," J. Chem. Eng. Jpn., 10, No. 1 (1977).
12. Mori, Hidzhikata, and Kuriyama, "Experimental study of the motion of a gas bubble in mercury in the presence and absence of a magnetic field," Trans. ASME Ser. C, 99, No. 3 (1977).
13. I. V. Belov, G. N. Elovikov, and B. E. Okulov, "Steady-state rate of rise of single bubbles in certain liquids," in: Heat and Mass Transfer Processes in the Baths of Steelmaking Furnaces [in Russian], Moscow (1974).
14. S. Uno and R. C. Kintner, "Effect of wall proximity on the rate of rise of single air bubbles in quiescent liquid," AIChE J., 2, No. 3 (1956).
15. P. H. Galderbank, D. S. L. Johnson, and I. Loudon, "Mechanics and mass transfer of single bubbles in free rise through some Newtonian and non-Newtonian liquids," Chem. Eng. Sci., 25, No. 2 (1970).